Frontiers of Information Technology & Electronic Engineering
www.jzus.zju.edu.cn; engineering.cae.cn; www.springerlink.com
ISSN 2095-9184 (print); ISSN 2095-9230 (online)
E-mail: jzus@zju.edu.cn

# Stability analysis of uncertain fractional-order neutral-type delay systems with actuator saturation

Zahra Sadat AGHAYAN[1], Alireza ALFI[†‡1], J. A. TENREIRO MACHADO[2]

[1]Faculty of Electrical and Robotic Engineering, Shahrood University of Technology, Shahrood 36199-95161, Iran

[2]Institute of Engineering, Polytechnic of Porto, Rua Dr. António Bernardino de Almeida 431, Porto 4249-015, Portugal

[†]E-mail: a_alfi@shahroodut.ac.ir

Received Aug. 30, 2020; Revision accepted Nov. 29, 2020; Crosschecked Aug. 6, 2021; Published online Sept. 18, 2021

**Abstract:** This study analyzes the problem of robust stability of fractional-order delay systems of neutral type under actuator saturation. A Lyapunov–Krasovskii (LK) function is constructed and conditions of the asymptotic robust stability of such systems are given, which are formulated by linear matrix inequalities (LMIs), using the Lyapunov direct method. An algorithm is introduced to compute the gain of the state feedback controller for extending the domain of attraction. The theoretical results are validated using some numerical examples.

**Key words:** Fractional-order system; Stability; Neutral delay; Robust; Saturation
https://doi.org/10.1631/FITEE.2000438 **CLC number:** O231

## 1 Introduction

Fractional calculus is the scientific area that addresses the theory of application integrals and derivatives with arbitrary non-integer order (Kilbas et al., 2000). Dynamic models involving fractional integrals and derivatives are called fractional-order (FO) systems. It has been reported that FO differential equations (FODEs) are valuable tools for modeling complex dynamics of physical systems in different fields of engineering, physics, and control (Pahnehkolaei et al., 2017a; Zhang Y et al., 2017; Dubey et al., 2020; Pu and Wang, 2020). Indeed, FODEs can more completely and concisely describe the behaviors of these systems than ordinary integer-order differential equations (IODEs), particularly in cases where there are responses with long memory transients (Baleanu et al., 2019a, 2019b; Yang et al., 2019). Accordingly, the stability of dynamic FO systems has become a key problem when considering real-world processes that are modeled with FODEs (Chen et al., 2017; Badri and Sojoodi, 2019c; Hu TT et al., 2020). Different FO system stability criteria have been discussed in the literature, including uniform stability (Pahnehkolaei et al., 2017b), Mittag–Leffler stability (Udhayakumar et al., 2020), and asymptotic stability (Binazadeh and Yousefi, 2018).

In addition, uncertainties in the dynamical models can strongly compromise the controller design procedure. There are different sources of uncertainties, such as variations in parameters, dynamical effects, and external disturbances. The modeling of real-world systems is never perfect and is often inaccurate due to un-modeled dynamics, ignored nonlinearities, perturbations of the physical parameters, and many other phenomena. Consequently, robust stability of the control systems, including FO systems, is of key importance (Zhang XF and Chen, 2018; Badri and Sojoodi, 2019b).

Delay is a prevalent and unavoidable effect in real systems due to the limited switching speed in electronic devices, which can degrade system

‡ Corresponding author
ORCID: Zahra Sadat AGHAYAN, https://orcid.org/0000-0002-8488-3685; Alireza ALFI, https://orcid.org/0000-0002-7034-0735; J. A. TENREIRO MACHADO, https://orcid.org/0000-0003-4274-4879

performance and even result in instabilities and oscillations. Hence, notable attention has been dedicated to address the stability of delayed dynamical systems, including the FO case (Badri and Sojoodi, 2019a; Mohsenipour and Fathi Jegarkandi, 2019; Pahnehkolaei et al., 2019b; Zhang S et al., 2019; He et al., 2020; Hu BX et al., 2020). Discussions of specific types of delay, such as neutral-type delay systems, can be found in the literature. A system that has delays in both the states and their derivatives is called a neutral-type delay system (Ren et al., 2017). We find neutral-type delay systems in different areas, such as networks with data loss (Lien et al., 2008), partial element equivalent circuits (Han, 2005), and population ecology (Barbarossa et al., 2014).

The development of FO delay systems led to a special focus on the neutral type (El Fezazi et al., 2017; Altun and Tunç, 2019; Li et al., 2019; Aghayan et al., 2020). It has also been reported that FO systems with neutral delay represent a more comprehensive class than other delay types (Liu MY et al., 2019; Chartbupapan et al., 2020). However, due to the derivative in the delayed state, the stability of such systems is still an open issue (Pahnehkolaei et al., 2019a). The input saturation constraint is also a key problem in the controller design. Control input saturation is a major issue in practice because actuator capabilities are limited. It is well known that input saturation can cause problems, but the stabilization problem and input saturation of FO systems have rarely been addressed together (Shahri et al., 2015, 2017, 2020; Alaviyan Shahri et al., 2018a, 2018b; Song et al., 2020; Zhu et al., 2020).

Motivated by the above discussions, it is crucial to study neutral delay in FO dynamic systems together with the input saturation and uncertainty. Here, the Lyapunov–Krasovskii (LK) function is constructed and we determine robust stability criteria expressed by linear matrix inequalities (LMIs) that are sufficient to achieve an appropriate state feedback control strategy. We also tackle the problem of finding a controller gain that can extend the domain of attraction.

Notations: The identity matrix with appropriate dimension is denoted by $\boldsymbol{I}$, the Euclidean vector norm or induced 2-norm of a matrix is denoted by $\|\cdot\|$, $\mathcal{C}_{\bar{h}}=\mathcal{C}\left(\left[\bar{h},0\right],\ \mathbb{R}^n\right)$ shows the Banach space mapping $\left[-\bar{h},0\right]\longrightarrow\mathbb{R}^n$ with the norm $\|\boldsymbol{Q}\|_c=\sup_{-\bar{h}\leq t\leq 0}\|\boldsymbol{Q}(t)\|$, the maximum eigenvalue of a matrix is represented as $\bar{\lambda}_{\max}(\cdot)$, and the symmetric part in a matrix is expressed by the symbol $*$.

## 2 Prerequisites and problem formulation

This section starts by reviewing definitions and lemmas that are useful in the rest of this paper. Then the problem is described in detail.

**Definition 1** (Valério et al., 2013) Given any function $f(t)\in C^{n+1}([t_0,+\infty),\ \mathbb{R})$, the Riemann–Liouville (RL) derivative is

$$\begin{aligned}{}^{\mathrm{RL}}_{t_0}\mathfrak{D}^{\alpha}_{t}f(t)=&\frac{1}{\Gamma(l-\alpha)}\frac{\mathrm{d}^l}{\mathrm{d}t^l}\int_{t_0}^{t}(t-s)^{l-\alpha-1}f(s)\mathrm{d}s,\\ &t\geq t_0,\ l\in\mathbb{Z}^+,\end{aligned}\tag{1}$$

where $\Gamma(\cdot)$ is the gamma function and $\alpha$ is the fractional order satisfying $0\leq l-1\leq\alpha<l$.

**Definition 2** (Valério et al., 2013) The RL integral of function $f(t)\in C^{n+1}([t_0,+\infty),\ \mathbb{R})$ with $\alpha>0$ is

$$I^{\alpha}f(t)=\frac{1}{\Gamma(\alpha)}\int_{t_0}^{t}(t-s)^{\alpha-1}f(s)\mathrm{d}s,\ t\geq t_0,\tag{2}$$

where $I$ is the RL integral of $f(t)$.

**Lemma 1** (Petersen, 1987) Assuming the real matrices with appropriate dimensions $\boldsymbol{\mathcal{H}}$, $\boldsymbol{\mathcal{Z}}$, and $\boldsymbol{\Pi}$ together with any $\boldsymbol{\mathcal{G}}(t)$ with $\boldsymbol{\mathcal{G}}^{\mathrm{T}}(t)\boldsymbol{\mathcal{G}}(t)\leq\boldsymbol{I}$, the following relationship holds:

$$\boldsymbol{\Pi}+\boldsymbol{\mathcal{H}}\boldsymbol{\mathcal{G}}(t)\boldsymbol{\mathcal{Z}}+\boldsymbol{\mathcal{Z}}^{\mathrm{T}}\boldsymbol{\mathcal{G}}^{\mathrm{T}}(t)\boldsymbol{\mathcal{H}}^{\mathrm{T}}<0,\tag{3}$$

if and only if

$$\boldsymbol{\Pi}+q\boldsymbol{\mathcal{H}}\boldsymbol{\mathcal{H}}^{\mathrm{T}}+q^{-1}\boldsymbol{\mathcal{Z}}^{\mathrm{T}}\boldsymbol{\mathcal{Z}}<0,\tag{4}$$

where the scalar $q>0$.

**Lemma 2** (Gu et al., 2003) For scalars $t_1$ and $t_2$ satisfying $t_2>t_1$, any positive definite matrix $\boldsymbol{R}$, and a vector function $\boldsymbol{\xi}:[t_1,t_2]\rightarrow\mathbb{R}^n$, the following inequality holds:

$$\begin{aligned}&(t_2-t_1)\int_{t_1}^{t_2}\boldsymbol{\xi}^{\mathrm{T}}(\delta)\boldsymbol{R}\boldsymbol{\xi}(\delta)\mathrm{d}\delta\\ &\geq\left(\int_{t_1}^{t_2}\boldsymbol{\xi}(\delta)\mathrm{d}\delta\right)^{\mathrm{T}}\boldsymbol{R}\left(\int_{t_1}^{t_2}\boldsymbol{\xi}(\delta)\mathrm{d}\delta\right).\end{aligned}\tag{5}$$

**Lemma 3** (Zhu et al., 2020) Suppose the set $\mathcal{S}(\breve{u}_0)=\{\breve{\boldsymbol{u}},\breve{\boldsymbol{v}}\mid\breve{\boldsymbol{u}},\breve{\boldsymbol{v}}\in\mathbb{R}^n,\ \|\breve{\boldsymbol{u}}-\breve{\boldsymbol{v}}\|\leq u_0\}$, in which $\breve{u}_0$ is the limit of saturation. If $\breve{\boldsymbol{v}}$ and $\breve{\boldsymbol{u}}$ are the elements of $\mathcal{S}$, using the dead-zone function $\boldsymbol{\psi}(\breve{\boldsymbol{u}}) = \breve{\boldsymbol{u}} - \text{sat}(\breve{\boldsymbol{u}})$, so that $\text{sat}(\breve{\boldsymbol{u}}) = \text{sign}(\breve{\boldsymbol{u}}) \cdot \min\{u_0, \|\breve{\boldsymbol{u}}\|\}$, then the following inequality holds:

$$\boldsymbol{\psi}^{\mathrm{T}}(\breve{\boldsymbol{u}})\,\boldsymbol{\Xi}\,[\boldsymbol{\psi}(\breve{\boldsymbol{u}}) - \breve{\boldsymbol{v}}] \le 0, \tag{6}$$

where the matrix $\boldsymbol{\Xi} \in \mathbb{R}^{m\times m}$ is positive diagonal, and sat($\cdot$) denotes the saturation.

**Lemma 4** (Liu S et al., 2016) Considering a vector of differentiable function $\boldsymbol{\xi}(t) \in \mathbb{R}^n$, for any constant symmetric positive semi-definite matrix $\boldsymbol{P} \in \mathbb{R}^{n\times n}$, we have

$$\begin{aligned}{}_{t_0}^{\mathrm{RL}}\mathfrak{D}_t^{\alpha}\left(\boldsymbol{\xi}^{\mathrm{T}}(t)\,\boldsymbol{P}\boldsymbol{\xi}(t)\right) \le & 2\boldsymbol{\xi}(t)\,\boldsymbol{P}\left({}_{t_0}^{\mathrm{RL}}\mathfrak{D}_t^{\alpha}\boldsymbol{\xi}(t)\right), \\ & \alpha \in (0,1). \end{aligned} \tag{7}$$

**Lemma 5** (Zhang FZ, 2006) Given the matrices $\boldsymbol{\Lambda}_1$, $\boldsymbol{\Lambda}_2$, and $\boldsymbol{\Lambda}_3$, where $\boldsymbol{\Lambda}_1 = {\boldsymbol{\Lambda}_1}^{\mathrm{T}}$ and $\boldsymbol{\Lambda}_2 > 0$, then $\boldsymbol{\Lambda}_1 + {\boldsymbol{\Lambda}_3}^{\mathrm{T}}{\boldsymbol{\Lambda}_2}^{-1}\boldsymbol{\Lambda}_3 < 0$ holds, if and only if

$$\begin{bmatrix}\boldsymbol{\Lambda}_1 & {\boldsymbol{\Lambda}_3}^{\mathrm{T}}\\ \boldsymbol{\Lambda}_3 & -\boldsymbol{\Lambda}_2\end{bmatrix} < 0 \text{ or } \begin{bmatrix}-\boldsymbol{\Lambda}_2 & \boldsymbol{\Lambda}_3\\ {\boldsymbol{\Lambda}_3}^{\mathrm{T}} & \boldsymbol{\Lambda}_1\end{bmatrix} < 0. \tag{8}$$

**Lemma 6** (Kilbas et al., 2006) If $\beta > q > 0$, then ${}_{t_0}^{\mathrm{RL}}\mathfrak{D}_t^{\beta}({}_{t_0}\mathfrak{D}_t^{-q}f(t)) = {}_{t_0}^{\mathrm{RL}}\mathfrak{D}_t^{\beta-q}f(t)$ holds for sufficiently good function $f(t)$. In particular, this relationship holds if $f(t)$ is integrable.

In this study, an uncertain FO neutral-type (FONT) delay system under input saturation considering $\alpha \in (0,1)$ is described in the dynamic equation

$$\begin{aligned}&{}_0^{\mathrm{RL}}\mathfrak{D}_t^{\alpha}\boldsymbol{\xi}(t) - (\boldsymbol{C} + \Delta\boldsymbol{C}(t)){}_0^{\mathrm{RL}}\mathfrak{D}_t^{\alpha}\boldsymbol{\xi}(t-h(t))\\ &=(\boldsymbol{A} + \Delta\boldsymbol{A}(t))\boldsymbol{\xi}(t) + (\boldsymbol{A}_0 + \Delta\boldsymbol{A}_0(t))\boldsymbol{\xi}(t-h(t))\\ &\quad + \boldsymbol{B}\boldsymbol{u}(t),\end{aligned} \tag{9}$$

with the initial conditions ${}_0^{\mathrm{RL}}\mathfrak{D}_t^{-(1-\alpha)}\boldsymbol{\xi}(t) = \boldsymbol{Q}(t)$, $t \in [-\bar{h}, 0]$, and $\boldsymbol{Q}(t) \in \mathcal{C}_{\bar{h}}$, where $\boldsymbol{\xi}(t) \in \mathbb{R}^n$ represents the state vector, $\boldsymbol{u}(t) \in \mathbb{R}^m$ shows the control input vector, and the real matrices $\boldsymbol{C}$, $\boldsymbol{A}$, $\boldsymbol{A}_0$, and $\boldsymbol{B}$ are constant with compatible dimensions. Additionally, the uncertainty terms are considered as

$$[\Delta\boldsymbol{A}(t)\ \ \Delta\boldsymbol{A}_0(t)\ \ \Delta\boldsymbol{C}(t)] = \boldsymbol{H}\boldsymbol{\mathcal{G}}(t)[\boldsymbol{F}_0\ \ \boldsymbol{F}_1\ \ \boldsymbol{F}_2], \tag{10}$$

where the real matrices $\boldsymbol{H}$, $\boldsymbol{F}_0$, $\boldsymbol{F}_1$, and $\boldsymbol{F}_2$ are known with compatible dimensions, and $\boldsymbol{\mathcal{G}}(t) \in \mathbb{R}^{n\times n}$, with $\boldsymbol{\mathcal{G}}^{\mathrm{T}}(t)\,\boldsymbol{\mathcal{G}}(t) \le \boldsymbol{I}$, represents the parameter uncertainties, which are time-varying. Furthermore, $h(t)$ denotes the unknown but bounded, continuous, and differentiable delay,

$$0 \le h(t) \le \bar{h}, \tag{11}$$

satisfying $\dot{h}(t) \le d < 1$. Here $d$ is the upper bound of derivation of $h(t)$.

Notice that this condition should be satisfied to ensure that the system to be controlled admits a physical meaningful solution that is compatible with the causality principle. For more information, see Witrant (2005). Furthermore, the matrix $\boldsymbol{Q}(t)$ is supposed to be continuously differentiable over $[-\bar{h}, 0]$:

$$\varkappa = \{\boldsymbol{Q}(t) \mid \boldsymbol{Q}(t) \in \mathcal{C}_{\bar{h}},\ \|\boldsymbol{Q}\|_c \le \rho_1,\ \|\dot{\boldsymbol{Q}}\|_c \le \rho_2\}, \tag{12}$$

where $\rho_1$ and $\rho_2$ are the positive scalars.

Let us consider the limited control input vector $\boldsymbol{u}$ as

$$\|\boldsymbol{u}_i\| \le u_{0i}, \tag{13}$$

where $u_{0i} > 0,\ i = 1, 2, \ldots, m$.

Assuming the state feedback controller $\boldsymbol{u}(t) = \boldsymbol{K}\boldsymbol{\xi}(t)$ and using inequality (13), the control signal is obtained as $\boldsymbol{u}(t) = \text{sat}(\boldsymbol{K}\boldsymbol{\xi}(t))$, where $u_i(t) = \text{sat}(\boldsymbol{K_i}\boldsymbol{\xi}(t)) = \text{sign}(\boldsymbol{K_i}\boldsymbol{\xi}(t)) \cdot \min\{u_{0i}, \|\boldsymbol{K_i}\boldsymbol{\xi}(t)\|\}$.

Accordingly, we can describe the FO system as

$$\begin{aligned}&{}_0^{\mathrm{RL}}\mathfrak{D}_t^{\alpha}\boldsymbol{\xi}(t) - (\boldsymbol{C} + \Delta\boldsymbol{C}(t)){}_0^{\mathrm{RL}}\mathfrak{D}_t^{\alpha}\boldsymbol{\xi}(t-h(t))\\ &=(\boldsymbol{A} + \Delta\boldsymbol{A}(t))\,\boldsymbol{\xi}(t) + (\boldsymbol{A}_0 + \Delta\boldsymbol{A}_0(t))\boldsymbol{\xi}(t-h(t))\\ &\quad + \boldsymbol{B}\text{sat}(\boldsymbol{K}\boldsymbol{\xi}(t)).\end{aligned} \tag{14}$$

If we define

$$\boldsymbol{\psi}(\boldsymbol{K}\boldsymbol{\xi}(t)) = \boldsymbol{K}\boldsymbol{\xi}(t) - \text{sat}(\boldsymbol{K}\boldsymbol{\xi}(t)), \tag{15}$$

where $\boldsymbol{\psi}(\boldsymbol{K}\boldsymbol{\xi}(t))$ denotes the dead-zone nonlinearity, then the overall FO system is expressed as

$$\begin{aligned}&{}_0^{\mathrm{RL}}\mathfrak{D}_t^{\alpha}\boldsymbol{\xi}(t) - (\boldsymbol{C} + \Delta\boldsymbol{C}(t)){}_0^{\mathrm{RL}}\mathfrak{D}_t^{\alpha}\boldsymbol{\xi}(t-h(t))\\ &=(\boldsymbol{A} + \Delta\boldsymbol{A}(t) + \boldsymbol{B}\boldsymbol{K})\,\boldsymbol{\xi}(t)\\ &\quad + (\boldsymbol{A}_0 + \Delta\boldsymbol{A}_0(t))\boldsymbol{\xi}(t-h(t)) - \boldsymbol{B}\boldsymbol{\psi}(\boldsymbol{K}\boldsymbol{\xi}(t)).\end{aligned} \tag{16}$$

## 3 Main results

Here, two theorems analyzing the stability of FONT system (16) are provided:

**Theorem 1** Let us consider any appropriate dimension matrices $\boldsymbol{\mu}_1$ and $\boldsymbol{\mu}_2$, the symmetric positive-definite matrices $\boldsymbol{P}$, $\boldsymbol{M}$, $\boldsymbol{N}$, and $\boldsymbol{Z}$, and a positive-definite diagonal matrix $\boldsymbol{\Lambda}$ satisfying the following LMIs:

$$\boldsymbol{\varGamma}=\begin{bmatrix}\boldsymbol{\varGamma}_{11} & * & * & * & * & * \\ \boldsymbol{\varGamma}_{21} & \boldsymbol{\varGamma}_{22} & * & * & * & * \\ \boldsymbol{\varGamma}_{31} & \boldsymbol{\varGamma}_{32} & \boldsymbol{\varGamma}_{33} & * & * & * \\ \boldsymbol{\varGamma}_{41} & \boldsymbol{\varGamma}_{42} & \boldsymbol{\varGamma}_{43} & \boldsymbol{\varGamma}_{44} & * & * \\ \boldsymbol{\varGamma}_{51} & \boldsymbol{\varGamma}_{52} & \boldsymbol{\varGamma}_{53} & \boldsymbol{\varGamma}_{54} & \boldsymbol{\varGamma}_{55} & * \\ \boldsymbol{\varGamma}_{61} & \boldsymbol{\varGamma}_{62} & \boldsymbol{\varGamma}_{63} & \boldsymbol{\varGamma}_{64} & \boldsymbol{\varGamma}_{65} & \boldsymbol{\varGamma}_{66}\end{bmatrix}<0, \tag{17}$$

where $\boldsymbol{\varGamma}_{11}=\boldsymbol{\mu_1 A}+\boldsymbol{A}^{\mathrm{T}}\boldsymbol{\mu}_1{}^{\mathrm{T}}+\boldsymbol{\mu}_1\boldsymbol{BK}+\boldsymbol{K}^{\mathrm{T}}\boldsymbol{B}^{\mathrm{T}}\boldsymbol{\mu}_1{}^{\mathrm{T}}+\boldsymbol{M}$, $\boldsymbol{\varGamma}_{21}=-\boldsymbol{\mu_1}^{\mathrm{T}}+\boldsymbol{\mu}_2\boldsymbol{A}+\boldsymbol{\mu}_2\boldsymbol{BK}+\boldsymbol{P}$, $\boldsymbol{\varGamma}_{22}=-\boldsymbol{\mu}_2-\boldsymbol{\mu}_2{}^{\mathrm{T}}+\bar{h}\boldsymbol{N}+\boldsymbol{Z}$, $\boldsymbol{\varGamma}_{31}=\boldsymbol{A}_0{}^{\mathrm{T}}\boldsymbol{\mu}_1{}^{\mathrm{T}}$, $\boldsymbol{\varGamma}_{32}=\boldsymbol{A}_0{}^{\mathrm{T}}\boldsymbol{\mu}_2{}^{\mathrm{T}}$, $\boldsymbol{\varGamma}_{33}=-(1-d)\boldsymbol{M}$, $\boldsymbol{\varGamma}_{41}=\boldsymbol{\varGamma}_{42}=\boldsymbol{\varGamma}_{43}=\mathbf{0}$, $\boldsymbol{\varGamma}_{44}=-\boldsymbol{N}/\bar{h}$, $\boldsymbol{\varGamma}_{51}=\boldsymbol{C}^{\mathrm{T}}\boldsymbol{\mu}_1{}^{\mathrm{T}}$, $\boldsymbol{\varGamma}_{52}=\boldsymbol{C}^{\mathrm{T}}\boldsymbol{\mu}_2{}^{\mathrm{T}}$, $\boldsymbol{\varGamma}_{53}=\boldsymbol{\varGamma}_{54}=\mathbf{0}$, $\boldsymbol{\varGamma}_{55}=-(1-d)\boldsymbol{Z}$, $\boldsymbol{\varGamma}_{61}=\boldsymbol{\varLambda G}-\boldsymbol{B}^{\mathrm{T}}\boldsymbol{\mu}_1{}^{\mathrm{T}}$, $\boldsymbol{\varGamma}_{62}=-\boldsymbol{B}^{\mathrm{T}}\boldsymbol{\mu}_2{}^{\mathrm{T}}$, $\boldsymbol{\varGamma}_{63}=\boldsymbol{\varGamma}_{64}=\boldsymbol{\varGamma}_{65}=\mathbf{0}$, $\boldsymbol{\varGamma}_{66}=-2\boldsymbol{\varLambda}$, and

$$\begin{aligned}\boldsymbol{\zeta}^{\mathrm{T}}=&\Big[\boldsymbol{\xi}^{\mathrm{T}}(t),\big({}_0^{\mathrm{RL}}\mathfrak{D}_t^{\alpha}\boldsymbol{\xi}(t)\big)^{\mathrm{T}},\boldsymbol{\xi}^{\mathrm{T}}(t-h(t)),\\&\int_{t-h(t)}^{t}\big({}_0^{\mathrm{RL}}\mathfrak{D}_t^{\alpha}\boldsymbol{\xi}(s)\big)^{\mathrm{T}}\mathrm{d}s,\\&\big({}_0^{\mathrm{RL}}\mathfrak{D}_t^{\alpha}\boldsymbol{\xi}(t-h(t))\big)^{\mathrm{T}},\boldsymbol{\psi}^{\mathrm{T}}(\boldsymbol{K\xi}(t))\Big].\end{aligned} \tag{18}$$

Then, system (16) with $\Delta\boldsymbol{A}(t)=\Delta\boldsymbol{A}_0(t)=\Delta\boldsymbol{C}(t)=\mathbf{0}$, that is, the nominal system, is asymptotically stable.

**Proof** We establish the LK function as

$$\begin{aligned}&V(t)\\=&{}_0^{\mathrm{RL}}\mathfrak{D}_t^{-(1-\alpha)}(\boldsymbol{\xi}^{\mathrm{T}}(t)\boldsymbol{P\xi}(t))\\&+\int_{t-h(t)}^{t}\boldsymbol{\xi}^{\mathrm{T}}(s)\boldsymbol{M\xi}(s)\mathrm{d}s\\&+\int_{-\bar{h}}^{0}\int_{t+\theta}^{t}\big({}_0^{\mathrm{RL}}\mathfrak{D}_t^{\alpha}\boldsymbol{\xi}(s)\big)^{\mathrm{T}}\boldsymbol{N}\big({}_0^{\mathrm{RL}}\mathfrak{D}_t^{\alpha}\boldsymbol{\xi}(s)\big)\mathrm{d}s\mathrm{d}\theta\\&+\int_{t-h(t)}^{t}\big({}_0^{\mathrm{RL}}\mathfrak{D}_t^{\alpha}\boldsymbol{\xi}(s)\big)^{\mathrm{T}}\boldsymbol{Z}\big({}_0^{\mathrm{RL}}\mathfrak{D}_t^{\alpha}\boldsymbol{\xi}(s)\big)\mathrm{d}s.\end{aligned} \tag{19}$$

Taking the time derivative of Eq. (19) results in the following:

$$\begin{aligned}&\dot{V}(t)\\=&{}_0^{\mathrm{RL}}\mathfrak{D}_t^{\alpha}\big(\boldsymbol{\xi}^{\mathrm{T}}(t)\boldsymbol{P\xi}(t)\big)+\boldsymbol{\xi}^{\mathrm{T}}(t)\boldsymbol{M\xi}(t)\\&-(1-d)\boldsymbol{\xi}^{\mathrm{T}}(t-h(t))\boldsymbol{M\xi}(t-h(t))\\&+\bar{h}\big({}_0^{\mathrm{RL}}\mathfrak{D}_t^{\alpha}\boldsymbol{\xi}(t)\big)^{\mathrm{T}}\boldsymbol{N}\big({}_0^{\mathrm{RL}}\mathfrak{D}_t^{\alpha}\boldsymbol{\xi}(t)\big)\\&-\int_{t-h(t)}^{t}\big({}_0^{\mathrm{RL}}\mathfrak{D}_t^{\alpha}\boldsymbol{\xi}(s)\big)^{\mathrm{T}}\boldsymbol{N}\big({}_0^{\mathrm{RL}}\mathfrak{D}_t^{\alpha}\boldsymbol{\xi}(s)\big)\mathrm{d}s\\&+\big({}_0^{RL}\mathfrak{D}_t^{\alpha}\boldsymbol{\xi}(t)\big)^{\mathrm{T}}\boldsymbol{Z}\big({}_0^{\mathrm{RL}}\mathfrak{D}_t^{\alpha}\boldsymbol{\xi}(t)\big)\\&-(1-d)\big({}_0^{\mathrm{RL}}\mathfrak{D}_t^{\alpha}\boldsymbol{\xi}(t-h(t))\big)^{\mathrm{T}}\boldsymbol{Z}\big({}_0^{\mathrm{RL}}\mathfrak{D}_t^{\alpha}\boldsymbol{\xi}(t-h(t))\big).\end{aligned} \tag{20}$$

Using Eq. (16) and applying the free weighting technique for matrices $\boldsymbol{\mu}_1$ and $\boldsymbol{\mu}_2$ with appropriate dimension yields

$$\begin{aligned}&2\Big[\boldsymbol{\xi}^{\mathrm{T}}(t)\mu_1+\big({}_0^{\mathrm{RL}}\mathfrak{D}_t^{\alpha}\boldsymbol{\xi}(t)\big)^{\mathrm{T}}\boldsymbol{\mu}_2\Big]\Big[-{}_0^{\mathrm{RL}}\mathfrak{D}_t^{\alpha}\boldsymbol{\xi}(t)\\&+\boldsymbol{C}{}_0^{\mathrm{RL}}\mathfrak{D}_t^{\alpha}\boldsymbol{\xi}(t-h(t))+(\boldsymbol{A}+\boldsymbol{BK})\boldsymbol{\xi}(t)\\&+\boldsymbol{A}_0\boldsymbol{\xi}(t-h(t))-\boldsymbol{B\psi}(\boldsymbol{K\xi}(t))\Big]=\mathbf{0}.\end{aligned} \tag{21}$$

In addition, it is straightforward that

$$\begin{aligned}&\dot{V}(t)\\\le&\dot{V}(t)-2\boldsymbol{\psi}^{\mathrm{T}}(\boldsymbol{K\xi}(t))\boldsymbol{\varLambda}[\boldsymbol{\psi}(\boldsymbol{K\xi}(t))-\boldsymbol{G\xi}(t)].\end{aligned} \tag{22}$$

Lemmas 2–4 and Eqs. (20) and (21) give

$$\begin{aligned}&\dot{V}(t)\\\le&2\boldsymbol{\xi}^{\mathrm{T}}(t)\boldsymbol{P}\big({}_0^{\mathrm{RL}}\mathfrak{D}_t^{\alpha}\boldsymbol{\xi}(t)\big)+\boldsymbol{\xi}^{\mathrm{T}}(t)\boldsymbol{M\xi}(t)\\&-(1-d)(\boldsymbol{\xi}^{\mathrm{T}}(t-h(t))\boldsymbol{M\xi}(t-h(t))\\&+\big({}_0^{\mathrm{RL}}\mathfrak{D}_t^{\alpha}\boldsymbol{\xi}(t-h(t))\big)^{\mathrm{T}}\boldsymbol{Z}\big({}_0^{\mathrm{RL}}\mathfrak{D}_t^{\alpha}\boldsymbol{\xi}(t-h(t))\big)\\&+\big({}_0^{\mathrm{RL}}\mathfrak{D}_t^{\alpha}\boldsymbol{\xi}(t)\big)^{\mathrm{T}}\big(\bar{h}\boldsymbol{N}+\boldsymbol{Z}\big)\big({}_0^{\mathrm{RL}}\mathfrak{D}_t^{\alpha}\boldsymbol{\xi}(t)\big)\\&-\left(\int_{t-h(t)}^{t}{}_0^{RL}\mathfrak{D}_t^{\alpha}\boldsymbol{\xi}(s)\mathrm{d}s\right)^{\mathrm{T}}\\&\cdot\frac{\boldsymbol{N}}{\bar{h}}\left(\int_{t-h(t)}^{t}{}_0^{\mathrm{RL}}\mathfrak{D}_t^{\alpha}\boldsymbol{\xi}(s)\mathrm{d}s\right)\\&+2\Big[\boldsymbol{\xi}^{\mathrm{T}}(t)\boldsymbol{\mu}_1+\big({}_0^{\mathrm{RL}}\mathfrak{D}_t^{\alpha}\boldsymbol{\xi}(t)\big)^{\mathrm{T}}\boldsymbol{\mu}_2\Big]\Big[-{}_0^{\mathrm{RL}}\mathfrak{D}_t^{\alpha}\boldsymbol{\xi}(t)\\&+\boldsymbol{C}{}_0^{\mathrm{RL}}\mathfrak{D}_t^{\alpha}\boldsymbol{\xi}(t-h(t))+(\boldsymbol{A}+\boldsymbol{BK})\boldsymbol{\xi}(t)\\&+\boldsymbol{A}_0\boldsymbol{\xi}(t-h(t))-\boldsymbol{B\psi}(\boldsymbol{K\xi}(t))\Big]\\&-2\boldsymbol{\psi}^{\mathrm{T}}(\boldsymbol{K\xi}(t))\boldsymbol{\varLambda}[\boldsymbol{\psi}(\boldsymbol{K\xi}(t))-\boldsymbol{G\xi}(t)].\end{aligned} \tag{23}$$

Simplifying inequality (23) yields the following:

$$\begin{aligned}&\dot{V}(t)\\\le&2\boldsymbol{\xi}^{\mathrm{T}}(t)\boldsymbol{P}\big({}_0^{\mathrm{RL}}\mathfrak{D}_t^{\alpha}\boldsymbol{\xi}(t)\big)+\boldsymbol{\xi}^{\mathrm{T}}(t)\boldsymbol{M\xi}(t)\\&-(1-d)\big(\boldsymbol{\xi}^{\mathrm{T}}(t-h(t))\boldsymbol{M\xi}(t-h(t))\big)\\&+\big({}_0^{\mathrm{RL}}\mathfrak{D}_t^{\alpha}\boldsymbol{\xi}(t-h(t))\big)^{\mathrm{T}}\boldsymbol{Z}\big({}_0^{\mathrm{RL}}\mathfrak{D}_t^{\alpha}\boldsymbol{\xi}(t-h(t))\big)\\&+\big({}_0^{\mathrm{RL}}\mathfrak{D}_t^{\alpha}\boldsymbol{\xi}(t)\big)^{\mathrm{T}}\big(\bar{h}\boldsymbol{N}+\boldsymbol{Z}\big)\big({}_0^{\mathrm{RL}}\mathfrak{D}_t^{\alpha}\boldsymbol{\xi}(t)\big)\\&-\left(\int_{t-h(t)}^{t}{}_0^{\mathrm{RL}}\mathfrak{D}_t^{\alpha}\boldsymbol{\xi}(s)\mathrm{d}s\right)^{\mathrm{T}}\\&\cdot\frac{\boldsymbol{N}}{\bar{h}}\left(\int_{t-h(t)}^{t}{}_0^{\mathrm{RL}}\mathfrak{D}_t^{\alpha}\boldsymbol{\xi}(s)\mathrm{d}s\right)\\&-2\boldsymbol{\xi}^{\mathrm{T}}(t)\boldsymbol{\mu}_1{}_0^{\mathrm{RL}}\mathfrak{D}_t^{\alpha}\boldsymbol{\xi}(t)\\&+2\boldsymbol{C\xi}^{\mathrm{T}}(t)\boldsymbol{\mu}_1{}_0^{\mathrm{RL}}\mathfrak{D}_t^{\alpha}\boldsymbol{\xi}(t-h(t))\end{aligned}$$

$$
\begin{aligned}
&+2\boldsymbol{\xi}^{\mathrm{T}}(t)\,\boldsymbol{\mu}_1(\boldsymbol{A}+\boldsymbol{BK})\,\boldsymbol{\xi}(t)\\
&+2\boldsymbol{\xi}^{\mathrm{T}}(t)\,\boldsymbol{\mu}_1\boldsymbol{A}_0\xi(t-h(t))\\
&-2\boldsymbol{\xi}^{\mathrm{T}}(t)\,\boldsymbol{\mu}_1\boldsymbol{B}\psi(\boldsymbol{K}\boldsymbol{\xi}(t))\\
&-2\left({}_0^{\mathrm{RL}}\mathfrak{D}_t^{\alpha}\boldsymbol{\xi}(t)\right)^{\mathrm{T}}\boldsymbol{\mu}_2\,{}_0^{\mathrm{RL}}\mathfrak{D}_t^{\alpha}\boldsymbol{\xi}(t)\\
&+2\left({}_0^{\mathrm{RL}}\mathfrak{D}_t^{\alpha}\boldsymbol{\xi}(t)\right)^{\mathrm{T}}\boldsymbol{\mu}_2\boldsymbol{C}{}_0^{\mathrm{RL}}\mathfrak{D}_t^{\alpha}\boldsymbol{\xi}(t-h(t))\\
&+2\left({}_0^{\mathrm{RL}}\mathfrak{D}_t^{\alpha}\boldsymbol{\xi}(t)\right)^{\mathrm{T}}\boldsymbol{\mu}_2(\boldsymbol{A}+\boldsymbol{BK})\,\boldsymbol{\xi}(t)\\
&+2\left({}_0^{\mathrm{RL}}\mathfrak{D}_t^{\alpha}\boldsymbol{\xi}(t)\right)^{\mathrm{T}}\boldsymbol{\mu}_2\boldsymbol{A}_0\boldsymbol{\xi}(t-h(t))\\
&-2\left({}_0^{\mathrm{RL}}\mathfrak{D}_t^{\alpha}\boldsymbol{\xi}(t)\right)^{\mathrm{T}}\boldsymbol{\mu}_2\boldsymbol{B}\psi(\boldsymbol{K}\boldsymbol{\xi}(t))\\
&-2\boldsymbol{\psi}^{\mathrm{T}}(\boldsymbol{K}\boldsymbol{\xi}(t))\,\boldsymbol{\Lambda}[\boldsymbol{\psi}(\boldsymbol{K}\boldsymbol{\xi}(t))-\boldsymbol{G}\boldsymbol{\xi}(t)]. \qquad (24)
\end{aligned}
$$

Using some algebraic manipulations, inequality (24) gives

$$\dot{V}(t) \le \boldsymbol{\zeta}^{\mathrm{T}}\boldsymbol{\Gamma}\boldsymbol{\zeta}, \qquad (25)$$

where

$$
\begin{aligned}
\boldsymbol{\zeta}^{\mathrm{T}} =\Bigg[&\boldsymbol{\xi}^{\mathrm{T}}(t),\left({}_0^{\mathrm{RL}}\mathfrak{D}_t^{\alpha}\boldsymbol{\xi}(t)\right)^{\mathrm{T}},\boldsymbol{\xi}^{\mathrm{T}}(t-h(t)),\\
&\int_{t-h(t)}^{t}\left({}_0^{\mathrm{RL}}\mathfrak{D}_t^{\alpha}\boldsymbol{\xi}(s)\right)^{\mathrm{T}}\mathrm{d}s,\\
&\left({}_0^{\mathrm{RL}}\mathfrak{D}_t^{\alpha}\boldsymbol{\xi}(t-h(t))\right)^{\mathrm{T}},\boldsymbol{\psi}^{\mathrm{T}}(\boldsymbol{K}\boldsymbol{\xi}(t))\Bigg], \qquad (26)
\end{aligned}
$$

and

$$
\boldsymbol{\Gamma}=\begin{bmatrix}
\boldsymbol{\Gamma}_{11} & * & * & * & * & *\\
\boldsymbol{\Gamma}_{21} & \boldsymbol{\Gamma}_{22} & * & * & * & *\\
\boldsymbol{\Gamma}_{31} & \boldsymbol{\Gamma}_{32} & \boldsymbol{\Gamma}_{33} & * & * & *\\
\boldsymbol{\Gamma}_{41} & \boldsymbol{\Gamma}_{42} & \boldsymbol{\Gamma}_{43} & \boldsymbol{\Gamma}_{44} & * & *\\
\boldsymbol{\Gamma}_{51} & \boldsymbol{\Gamma}_{52} & \boldsymbol{\Gamma}_{53} & \boldsymbol{\Gamma}_{54} & \boldsymbol{\Gamma}_{55} & *\\
\boldsymbol{\Gamma}_{61} & \boldsymbol{\Gamma}_{62} & \boldsymbol{\Gamma}_{63} & \boldsymbol{\Gamma}_{64} & \boldsymbol{\Gamma}_{65} & \boldsymbol{\Gamma}_{66}
\end{bmatrix}, \qquad (27)
$$

with $\boldsymbol{\Gamma}_{11}=\boldsymbol{\mu}_1\boldsymbol{A}+\boldsymbol{A}^{\mathrm{T}}{\boldsymbol{\mu}_1}^{\mathrm{T}}+\boldsymbol{\mu}_1\boldsymbol{BK}+\boldsymbol{K}^{\mathrm{T}}\boldsymbol{B}^{\mathrm{T}}{\boldsymbol{\mu}_1}^{\mathrm{T}}+\boldsymbol{M}$, $\boldsymbol{\Gamma}_{21}=-{\boldsymbol{\mu}_1}^{\mathrm{T}}+\boldsymbol{\mu}_2\boldsymbol{A}+\boldsymbol{\mu}_2\boldsymbol{BK}+\boldsymbol{P}$, $\boldsymbol{\Gamma}_{22}=-\boldsymbol{\mu}_2-{\boldsymbol{\mu}_2}^{\mathrm{T}}+\bar{h}\boldsymbol{N}+\boldsymbol{Z}$, $\boldsymbol{\Gamma}_{31}={\boldsymbol{A}_0}^{\mathrm{T}}{\boldsymbol{\mu}_1}^{\mathrm{T}}$, $\boldsymbol{\Gamma}_{32}={\boldsymbol{A}_0}^{\mathrm{T}}{\boldsymbol{\mu}_2}^{\mathrm{T}}$, $\boldsymbol{\Gamma}_{33}=-(1-d)\,\boldsymbol{M}$, $\boldsymbol{\Gamma}_{41}=\boldsymbol{\Gamma}_{42}=\boldsymbol{\Gamma}_{43}=\boldsymbol{0}$, $\boldsymbol{\Gamma}_{44}=-\boldsymbol{N}/\bar{h}$, $\boldsymbol{\Gamma}_{51}=\boldsymbol{C}^{\mathrm{T}}{\boldsymbol{\mu}_1}^{\mathrm{T}}$, $\boldsymbol{\Gamma}_{52}=\boldsymbol{C}^{\mathrm{T}}{\boldsymbol{\mu}_2}^{\mathrm{T}}$, $\boldsymbol{\Gamma}_{53}=\boldsymbol{\Gamma}_{54}=\boldsymbol{0}$, $\boldsymbol{\Gamma}_{55}=-(1-d)\,\boldsymbol{Z}$, $\boldsymbol{\Gamma}_{61}=\boldsymbol{\Lambda}\boldsymbol{G}-\boldsymbol{B}^{\mathrm{T}}{\boldsymbol{\mu}_1}^{\mathrm{T}}$, $\boldsymbol{\Gamma}_{62}=-\boldsymbol{B}^{\mathrm{T}}{\boldsymbol{\mu}_2}^{\mathrm{T}}$, $\boldsymbol{\Gamma}_{63}=\boldsymbol{\Gamma}_{64}=\boldsymbol{\Gamma}_{65}=\boldsymbol{0}$, and $\boldsymbol{\Gamma}_{66}=-2\boldsymbol{\Lambda}$. Hence, $\dot{V}(t)<0$ if the above LMIs hold, which verifies the convergence of the nominal FONT trajectories asymptotic to the origin.

**Theorem 2** Let us consider the positive scalars $q$, $\beta$, and $\rho$, a diagonal matrix $\boldsymbol{R}$ with appropriate dimension, the symmetric positive-definite matrices $\bar{\boldsymbol{M}}$, $\bar{\boldsymbol{N}}$, $\bar{\boldsymbol{P}}$, and $\bar{\boldsymbol{Z}}$, the matrices $\boldsymbol{X}$, $\boldsymbol{U}$, and $\boldsymbol{L}$ with compatible dimensions, and a real scalar $\gamma$ satisfying the conditions

$$
\begin{bmatrix}
\boldsymbol{\Phi} & * & * & * & * & * & *\\
\boldsymbol{\vartheta} & \boldsymbol{\Theta} & * & * & * & * & *\\
\boldsymbol{\Xi}_{31} & \boldsymbol{\Xi}_{32} & \boldsymbol{\Xi}_{33} & * & * & * & *\\
\boldsymbol{\Xi}_{41} & \boldsymbol{\Xi}_{42} & \boldsymbol{\Xi}_{43} & \boldsymbol{\Xi}_{44} & * & * & *\\
\boldsymbol{\Xi}_{51} & \boldsymbol{\Xi}_{52} & \boldsymbol{\Xi}_{53} & \boldsymbol{\Xi}_{54} & \boldsymbol{\Xi}_{55} & * & *\\
\boldsymbol{\Xi}_{61} & \boldsymbol{\Xi}_{62} & \boldsymbol{\Xi}_{63} & \boldsymbol{\Xi}_{64} & \boldsymbol{\Xi}_{65} & \boldsymbol{\Xi}_{66} & *\\
\boldsymbol{F}_0\boldsymbol{X}^{\mathrm{T}} & \boldsymbol{0} & \boldsymbol{F}_1\boldsymbol{X}^{\mathrm{T}} & \boldsymbol{0} & \boldsymbol{F}_2\boldsymbol{X}^{\mathrm{T}} & \boldsymbol{0} & -q\boldsymbol{I}
\end{bmatrix}
< 0, \qquad (28)
$$

where $\boldsymbol{\Phi}=\boldsymbol{\Xi}_{11}+q\boldsymbol{H}\boldsymbol{H}^{\mathrm{T}}$, $\boldsymbol{\vartheta}=\boldsymbol{\Xi}_{21}+\gamma q\boldsymbol{H}\boldsymbol{H}^{\mathrm{T}}$, $\boldsymbol{\Theta}=\boldsymbol{\Xi}_{22}+\gamma^2 q\boldsymbol{H}\boldsymbol{H}^{\mathrm{T}}$, $\boldsymbol{\Xi}_{11}=\boldsymbol{A}\boldsymbol{X}^{\mathrm{T}}+\boldsymbol{X}\boldsymbol{A}^{\mathrm{T}}+\boldsymbol{BU}+\boldsymbol{U}^{\mathrm{T}}\boldsymbol{B}^{\mathrm{T}}+\bar{\boldsymbol{M}}$, $\boldsymbol{\Xi}_{21}=-\boldsymbol{X}+\gamma\boldsymbol{A}\boldsymbol{X}^{\mathrm{T}}+\gamma\boldsymbol{BU}+\bar{\boldsymbol{P}}$, $\boldsymbol{\Xi}_{22}=-\gamma\boldsymbol{X}-\gamma\boldsymbol{X}^{\mathrm{T}}+\bar{h}\,\bar{\boldsymbol{N}}+\bar{\boldsymbol{Z}}$, $\boldsymbol{\Xi}_{31}=\boldsymbol{X}{\boldsymbol{A}_0}^{\mathrm{T}}$, $\boldsymbol{\Xi}_{32}=\gamma\boldsymbol{X}{\boldsymbol{A}_0}^{\mathrm{T}}$, $\boldsymbol{\Xi}_{33}=-(1-d)\bar{\boldsymbol{M}}$, $\boldsymbol{\Xi}_{41}=\boldsymbol{\Xi}_{42}=\boldsymbol{\Xi}_{43}=\boldsymbol{0}$, $\boldsymbol{\Xi}_{44}=-\bar{\boldsymbol{N}}/\bar{h}$, $\boldsymbol{\Xi}_{51}=\boldsymbol{X}\boldsymbol{C}^{\mathrm{T}}$, $\boldsymbol{\Xi}_{52}=\gamma\boldsymbol{X}\boldsymbol{C}^{\mathrm{T}}$, $\boldsymbol{\Xi}_{53}=\boldsymbol{\Xi}_{54}=\boldsymbol{0}$, $\boldsymbol{\Xi}_{55}=-(1-d)\bar{\boldsymbol{Z}}$, $\boldsymbol{\Xi}_{61}=\boldsymbol{L}-\boldsymbol{R}\boldsymbol{B}^{\mathrm{T}}$, $\boldsymbol{\Xi}_{62}=-\gamma\boldsymbol{R}\boldsymbol{B}^{\mathrm{T}}$, $\boldsymbol{\Xi}_{63}=\boldsymbol{\Xi}_{64}=\boldsymbol{\Xi}_{65}=\boldsymbol{0}$, and $\boldsymbol{\Xi}_{66}=-2\boldsymbol{R}^{\mathrm{T}}$,

$$
\begin{bmatrix}
\bar{\boldsymbol{P}} & *\\
\boldsymbol{U}_i-\boldsymbol{L}_i & \beta{u_{0i}}^2
\end{bmatrix} \ge 0,\ i=1,2,\ldots,m, \qquad (29)
$$

$$
\begin{aligned}
&\left(\bar{h}\bar{\lambda}_{\max}\left(\boldsymbol{X}^{-1}\bar{\boldsymbol{M}}\boldsymbol{X}^{-\mathrm{T}}\right)+\bar{\lambda}_{\max}\left(\boldsymbol{X}^{-1}\bar{\boldsymbol{P}}\boldsymbol{X}^{-\mathrm{T}}\right)\right)||\boldsymbol{Q}||_c^2\\
&+\left(\frac{\bar{h}^2}{2}\bar{\lambda}_{\max}\left(\boldsymbol{X}^{-1}\bar{\boldsymbol{N}}\boldsymbol{X}^{-\mathrm{T}}\right)\right.\\
&\left.+\bar{h}\,\bar{\lambda}_{\max}\left(\boldsymbol{X}^{-1}\bar{\boldsymbol{Z}}\boldsymbol{X}^{-\mathrm{T}}\right)\right)||\dot{\boldsymbol{Q}}||_c^2 \le \beta^{-1}. \qquad (30)
\end{aligned}
$$

Then, applying the gain of controller $\boldsymbol{K}=\boldsymbol{U}\boldsymbol{X}^{-\mathrm{T}}$, the FONT system given in (16) is asymptotically robustly stable.

**Proof** We consider $\boldsymbol{\mu}_2=\gamma\boldsymbol{\mu}_1$, $\gamma>0$. Multiplying inequality (17) by diag(${\boldsymbol{\mu}_1}^{-1}$, ${\boldsymbol{\mu}_1}^{-1}$, ${\boldsymbol{\mu}_1}^{-1}$, ${\boldsymbol{\mu}_1}^{-1}$, ${\boldsymbol{\mu}_1}^{-1}$, $\boldsymbol{\Lambda}^{-1}$) on the left and its transpose on the right, and considering $\boldsymbol{L}=\boldsymbol{G}\boldsymbol{X}^{\mathrm{T}}$, $\boldsymbol{U}=\boldsymbol{K}\boldsymbol{X}^{\mathrm{T}}$, $\boldsymbol{X}={\boldsymbol{\mu}_1}^{-1}$, $\boldsymbol{R}=\boldsymbol{\Lambda}^{-1}$, and $=\boldsymbol{X}\boldsymbol{\Omega}\boldsymbol{X}^{\mathrm{T}}$, in which $\boldsymbol{\Omega}=\boldsymbol{P},\boldsymbol{Z},\boldsymbol{N},\boldsymbol{M}$, we obtain

$$
\boldsymbol{\Xi}=\begin{bmatrix}
\boldsymbol{\Xi}_{11} & * & * & * & * & *\\
\boldsymbol{\Xi}_{21} & \boldsymbol{\Xi}_{22} & * & * & * & *\\
\boldsymbol{\Xi}_{31} & \boldsymbol{\Xi}_{32} & \boldsymbol{\Xi}_{33} & * & * & *\\
\boldsymbol{\Xi}_{41} & \boldsymbol{\Xi}_{42} & \boldsymbol{\Xi}_{43} & \boldsymbol{\Xi}_{44} & * & *\\
\boldsymbol{\Xi}_{51} & \boldsymbol{\Xi}_{52} & \boldsymbol{\Xi}_{53} & \boldsymbol{\Xi}_{54} & \boldsymbol{\Xi}_{55} & *\\
\boldsymbol{\Xi}_{61} & \boldsymbol{\Xi}_{62} & \boldsymbol{\Xi}_{63} & \boldsymbol{\Xi}_{64} & \boldsymbol{\Xi}_{65} & \boldsymbol{\Xi}_{66}
\end{bmatrix} < 0. \qquad (31)
$$

Considering the uncertainty and applying Eq. (10), $\boldsymbol{A}$, $\boldsymbol{A}_0$, and $\boldsymbol{C}$ are replaced by $\boldsymbol{A}+$

$\boldsymbol{H}\boldsymbol{\mathcal{G}}(t)\boldsymbol{F}_0$, $\boldsymbol{A}_0 + \boldsymbol{H}\boldsymbol{\mathcal{G}}(t)\boldsymbol{F}_1$, and $\boldsymbol{C} + \boldsymbol{H}\boldsymbol{\mathcal{G}}(t)\boldsymbol{F}_2$, respectively. Inequality (31) is equivalent to

$$\boldsymbol{\varXi} + \begin{bmatrix} \boldsymbol{H} \\ \gamma\boldsymbol{H} \\ \boldsymbol{0} \\ \boldsymbol{0} \\ \boldsymbol{0} \\ \boldsymbol{0} \end{bmatrix} \boldsymbol{\mathcal{G}}(t)\left[\boldsymbol{F}_0\boldsymbol{X}^{\mathrm{T}}\ \ \boldsymbol{0}\ \ \boldsymbol{F}_1\boldsymbol{X}^{\mathrm{T}}\ \ \boldsymbol{0}\ \ \boldsymbol{F}_2\boldsymbol{X}^{\mathrm{T}}\ \ \boldsymbol{0}\right] + \begin{bmatrix} \boldsymbol{X}\boldsymbol{F}_0{}^{\mathrm{T}} \\ \boldsymbol{0} \\ \boldsymbol{X}\boldsymbol{F}_1{}^{\mathrm{T}} \\ \boldsymbol{0} \\ \boldsymbol{X}\boldsymbol{F}_2{}^{\mathrm{T}} \\ \boldsymbol{0} \end{bmatrix} \boldsymbol{\mathcal{G}}^{\mathrm{T}}(t)\left[\boldsymbol{H}^{\mathrm{T}}\ \ \gamma\boldsymbol{H}^{\mathrm{T}}\ \ \boldsymbol{0}\ \ \boldsymbol{0}\ \ \boldsymbol{0}\ \ \boldsymbol{0}\right] < 0. \tag{32}$$

Using Lemmas 1 and 5, after some manipulations, we obtain the conditions in inequality (28).

For a scalar $\beta > 0$, the ellipsoid $\mathcal{D}_{\mathrm{e}}$ is defined as

$$\mathcal{D}_{\mathrm{e}} = \Big\{\boldsymbol{\xi}(t) \mid \boldsymbol{\xi}(t) \in \mathbb{R}^n,\ {}_0^{\mathrm{RL}}\mathfrak{D}_t^{-(1-\alpha)}\left(\boldsymbol{\xi}^{\mathrm{T}}(t)\boldsymbol{P}\boldsymbol{\xi}(t)\right) \le \beta^{-1}\Big\}. \tag{33}$$

Inequality (29) guarantees that $\forall\ \boldsymbol{\xi} \in \mathcal{D}_{\mathrm{e}}$, $\boldsymbol{\xi} \in \mathcal{S}$. Indeed, $\mathcal{D}_{\mathrm{e}} \subset \mathcal{S}$ is verified by

$$\begin{bmatrix} \boldsymbol{P} & * \\ \boldsymbol{K}_i - \boldsymbol{G}_i & \beta {u_{0i}}^2 \end{bmatrix} \ge 0. \tag{34}$$

Pre- and post-multiplying inequality (34) by $\boldsymbol{\varPi} = \mathrm{diag}(\boldsymbol{X},\ \boldsymbol{I})$ and $\boldsymbol{\varPi}^{\mathrm{T}}$, respectively, inequality (34) yields

$$\begin{aligned} &\begin{bmatrix} \boldsymbol{X} & \boldsymbol{0} \\ \boldsymbol{0} & \boldsymbol{I} \end{bmatrix} \begin{bmatrix} \boldsymbol{P} & * \\ \boldsymbol{K}_i - \boldsymbol{G}_i & \beta {u_{0i}}^2 \end{bmatrix} \begin{bmatrix} \boldsymbol{X}^{\mathrm{T}} & \boldsymbol{0} \\ \boldsymbol{0} & \boldsymbol{I} \end{bmatrix} \\ &= \begin{bmatrix} \boldsymbol{X}\boldsymbol{P}\boldsymbol{X}^{\mathrm{T}} & * \\ \boldsymbol{K}_i\boldsymbol{X}^{\mathrm{T}} - \boldsymbol{G}_i\boldsymbol{X}^{\mathrm{T}} & \beta {u_{0i}}^2 \end{bmatrix} \\ &= \begin{bmatrix} \bar{\boldsymbol{P}} & * \\ \boldsymbol{U}_i - \boldsymbol{L}_i & \beta {u_{0i}}^2 \end{bmatrix}. \end{aligned} \tag{35}$$

In addition, using Eq. (19), we have

$$\begin{aligned} &V(0) \\ &\le {}_0^{RL}\mathfrak{D}_t^{-(1-\alpha)}\left(\boldsymbol{\xi}^{\mathrm{T}}(0)\boldsymbol{P}\boldsymbol{\xi}(0)\right) \\ &\quad + \int_{-\bar{h}}^{0} \boldsymbol{\xi}^{\mathrm{T}}(s)\boldsymbol{M}\boldsymbol{\xi}(s)\,\mathrm{d}s \\ &\quad + \int_{-\bar{h}}^{0}\int_{\theta}^{0} \left({}_0^{\mathrm{RL}}\mathfrak{D}_t^{\alpha}\boldsymbol{\xi}(s)\right)^{\mathrm{T}}\boldsymbol{N}\left({}_0^{\mathrm{RL}}\mathfrak{D}_t^{\alpha}\boldsymbol{\xi}(s)\right)\mathrm{d}s\mathrm{d}\theta \\ &\quad + \int_{-\bar{h}}^{0} \left({}_0^{\mathrm{RL}}\mathfrak{D}_t^{\alpha}\boldsymbol{\xi}(s)\right)^{\mathrm{T}}\boldsymbol{Z}\left({}_0^{\mathrm{RL}}\mathfrak{D}_t^{\alpha}\boldsymbol{\xi}(s)\right)\mathrm{d}s \\ &\le \left(\bar{\lambda}_{\max}(\boldsymbol{P}) + \bar{h}\,\bar{\lambda}_{\max}(\boldsymbol{M})\right) \parallel \boldsymbol{Q} \parallel_c^2 \\ &\quad + \left(\frac{\bar{h}^2}{2}\bar{\lambda}_{\max}(\boldsymbol{N}) + \bar{h}\,\bar{\lambda}_{\max}(\boldsymbol{Z})\right) \parallel \dot{\boldsymbol{Q}} \parallel_c^2 = \rho. \end{aligned} \tag{36}$$

Therefore, we have ${}_0^{\mathrm{RL}}\mathfrak{D}_t^{-(1-\alpha)}\left(\boldsymbol{\xi}^{\mathrm{T}}(t)\boldsymbol{P}\boldsymbol{\xi}(t)\right) \le V(t) \le V(0) \le \rho \le \beta^{-1}$.

In other words, the system trajectories do not leave the set $\mathcal{D}_{\mathrm{e}}$ for any initial function $\boldsymbol{Q}(t) \in \mathcal{D}_{\mathrm{e}}$ ensuring $\boldsymbol{\xi}(t) \in \mathcal{S}$.

**Remark 1** Because inequality (30) is nonlinear, it cannot be solved using the LMI toolbox. Hence, we need to apply the cone complementarity linearization (CCL) method.

**Remark 2** A key topic in controller design is determining the controller gains for extending the domain of attraction. We address this problem in the next section.

## 4 Extension of the domain of attraction

We specify the state feedback controller gain to extend the domain of attraction while the robust stability of system (16) is guaranteed. The extension of the domain of attraction is accomplished while taking into account conditions of the eigenvalues $\tilde{\boldsymbol{X}}\tilde{\boldsymbol{M}}\tilde{\boldsymbol{X}}^{\mathrm{T}}$, $\tilde{\boldsymbol{X}}\tilde{\boldsymbol{P}}\tilde{\boldsymbol{X}}^{\mathrm{T}}$, $\tilde{\boldsymbol{X}}\tilde{\boldsymbol{N}}\tilde{\boldsymbol{X}}^{\mathrm{T}}$, and $\tilde{\boldsymbol{X}}\tilde{\boldsymbol{Z}}\tilde{\boldsymbol{X}}^{\mathrm{T}}$:

$$\begin{bmatrix} \upsilon_1\boldsymbol{I} & \tilde{\boldsymbol{X}} \\ \tilde{\boldsymbol{X}}^{\mathrm{T}} & \tilde{\boldsymbol{P}} \end{bmatrix} \ge 0,\ \begin{bmatrix} \upsilon_2\boldsymbol{I} & \tilde{\boldsymbol{X}} \\ \tilde{\boldsymbol{X}}^{\mathrm{T}} & \tilde{\boldsymbol{M}} \end{bmatrix} \ge 0,\ \begin{bmatrix} \upsilon_3\boldsymbol{I} & \tilde{\boldsymbol{X}} \\ \tilde{\boldsymbol{X}}^{\mathrm{T}} & \tilde{\boldsymbol{N}} \end{bmatrix} \ge 0,\ \begin{bmatrix} \upsilon_4\boldsymbol{I} & \tilde{\boldsymbol{X}} \\ \tilde{\boldsymbol{X}}^{\mathrm{T}} & \tilde{\boldsymbol{Z}} \end{bmatrix} \ge 0. \tag{37}$$

The condition given in inequality (30) is satisfied if the following inequality holds:

$$\left[\upsilon_1 + \bar{h}\upsilon_2 + \frac{\bar{h}^2}{2}\upsilon_3 + \bar{h}\upsilon_4\right]\rho^2 \le \beta^{-1}, \tag{38}$$

where $\rho^2 = \max\left(\|\boldsymbol{Q}(t)\|_c^2,\ \|\dot{\boldsymbol{Q}}(t)\|_c^2\right)$, $\tilde{\boldsymbol{\Omega}} = \bar{\boldsymbol{\Omega}}^{-1}$ with $\boldsymbol{\Omega} = \boldsymbol{N}, \boldsymbol{Z}, \boldsymbol{M}, \boldsymbol{P}$, and $\tilde{\boldsymbol{X}} = \boldsymbol{X}^{-1}$. Here, the stability radius $\rho$ must be computed. Now, for the prescribed values of $\bar{h}$, the feasibility problem can be written as follows: Find $\bar{\boldsymbol{Z}}$, $\bar{\boldsymbol{N}}$, $\bar{\boldsymbol{M}}$, $\bar{\boldsymbol{P}}$, $\tilde{\boldsymbol{P}}$, $\tilde{\boldsymbol{M}}$, $\tilde{\boldsymbol{N}}$, $\tilde{\boldsymbol{Z}}$, $\tilde{\boldsymbol{X}}$, $\boldsymbol{X}$, $\upsilon_j$ $(j = 1, 2, 3, 4)$, s.t. $\bar{\boldsymbol{\Omega}} > 0$, $\tilde{\boldsymbol{\Omega}} > 0$, $\beta > 0$, $\rho > 0$, $\upsilon_i > 0$, and inequalities (28), (29), (37), and (38) are satisfied.

If a feasible solution can be found for the problem mentioned above and for the prescribed $\bar{h}$, then we conclude that a controller can be designed which ensures the robust stability of the FONT system with arbitrary initial states in $\varkappa$. Notice that due to nonlinear conditions in the above problem, we cannot adopt the LMI toolbox directly. This problem can be converted into the following LMI conditions:

$$\begin{aligned}
&\min \operatorname{tr}\{\bar{\boldsymbol{M}}\tilde{\boldsymbol{M}} + \bar{\boldsymbol{P}}\tilde{\boldsymbol{P}} + \bar{\boldsymbol{N}}\tilde{\boldsymbol{N}} + \bar{\boldsymbol{Z}}\tilde{\boldsymbol{Z}} \\
&\qquad + (\boldsymbol{X} + \boldsymbol{X}^{\mathrm{T}})(\tilde{\boldsymbol{X}} + \tilde{\boldsymbol{X}}^{\mathrm{T}})\}, \\
&\text{s.t.} \begin{bmatrix} \bar{\boldsymbol{M}} & * \\ \boldsymbol{I} & \tilde{\boldsymbol{M}} \end{bmatrix} \geq 0, \begin{bmatrix} \bar{\boldsymbol{P}} & * \\ \boldsymbol{I} & \tilde{\boldsymbol{P}} \end{bmatrix} \geq 0, \begin{bmatrix} \bar{\boldsymbol{N}} & * \\ \boldsymbol{I} & \tilde{\boldsymbol{N}} \end{bmatrix} \geq 0, \\
&\begin{bmatrix} \bar{\boldsymbol{Z}} & * \\ \boldsymbol{I} & \tilde{\boldsymbol{Z}} \end{bmatrix} \geq 0, \begin{bmatrix} \boldsymbol{X} + \boldsymbol{X}^{\mathrm{T}} & * \\ \boldsymbol{I} & \tilde{\boldsymbol{X}} + \tilde{\boldsymbol{X}}^{\mathrm{T}} \end{bmatrix} \geq 0.
\end{aligned} \tag{39}$$

The procedure to determine the controller gain using the CCL method (Elahi and Alfi, 2017) can be summarized as follows:

1. For given $\bar{h}$ and $\beta$, and the initial values $\gamma = \gamma_0$, select a sufficiently large initial value of $\rho$ so that a feasible solution for LMI conditions (39) exists.

2. Compute a feasible solution $\bar{\boldsymbol{\Omega}}_0$, $\tilde{\boldsymbol{\Omega}}_0$, $\boldsymbol{X}_0$, and $\tilde{\boldsymbol{X}}_0$ satisfying LMI conditions (39).

3. Solve the following problem:

$$\begin{aligned}
&\min \operatorname{tr}\{\bar{\boldsymbol{M}}\tilde{\boldsymbol{M}}_0 + \bar{\boldsymbol{P}}\tilde{\boldsymbol{P}}_0 + \bar{\boldsymbol{N}}\tilde{\boldsymbol{N}}_0 + \bar{\boldsymbol{Z}}\tilde{\boldsymbol{Z}}_0 \\
&+ (\boldsymbol{X} + \boldsymbol{X}^{\mathrm{T}})(\tilde{\boldsymbol{X}}_0 + \tilde{\boldsymbol{X}}_0^{\mathrm{T}}) + \bar{\boldsymbol{P}}\tilde{\boldsymbol{P}}_0 + \bar{\boldsymbol{M}}_0\tilde{\boldsymbol{M}} + \bar{\boldsymbol{N}}_0\tilde{\boldsymbol{N}} \\
&+ \bar{\boldsymbol{Z}}_0\tilde{\boldsymbol{Z}} + (\boldsymbol{X}_0 + \boldsymbol{X}_0^{\mathrm{T}})(\tilde{\boldsymbol{X}} + \tilde{\boldsymbol{X}}^{\mathrm{T}})\},
\end{aligned}$$

considering the LMI conditions (39).

4. Substitute the updated matrices $\bar{\boldsymbol{P}}$, $\bar{\boldsymbol{M}}$, $\bar{\boldsymbol{N}}$, $\bar{\boldsymbol{Z}}$, $\tilde{\boldsymbol{P}}$, $\tilde{\boldsymbol{M}}$, $\tilde{\boldsymbol{N}}$, $\tilde{\boldsymbol{Z}}$, $\boldsymbol{X}$, and $\tilde{\boldsymbol{X}}$ from step 3. If the solution is not feasible, then set the new matrices to be $\tilde{\boldsymbol{\Omega}}_0$, $\bar{\boldsymbol{\Omega}}_0$, $\tilde{\boldsymbol{X}}_0$, and $\boldsymbol{X}_0$ and go to the previous step. Otherwise, consider $\rho_0 = \rho$ and $\gamma_0 = \gamma$.

**Remark 3** For the prescribed values of $\bar{h}$ and $d$, the maximal domain of attraction can be achieved by increasing $\rho$ while ensuring the robust stability of the FONT system.

## 5 Application

In this section, we discuss how the obtained theoretical results can be used in practical applications. For this purpose, we consider one example, namely the wind tunnel.

A dynamic model of the wind tunnel is given by (Manitius, 1984)

$$\begin{cases} \dfrac{1}{a}\delta\dot{M}(t) + \delta M(t) = k\delta\theta(t - h(t)), \\ \delta\ddot{\theta}(t) + 2\varsigma\omega\delta\dot{\theta}(t) + \omega^2\delta\theta(t) = \omega^2\delta\theta_a(t), \end{cases} \tag{40}$$

where $\delta\theta$ is the guide vane angle, $a$, $k$, $\varsigma$, and $\omega$ are the constant parameters depending on the operating point, and $\delta\theta$ and $\delta\dot{\theta}$ represent the guide vane angle and its variation rate, respectively. Moreover, $\delta M$ denotes the variation in the Mach number, and $h(t)$ represents the delay of the transportation between the fan and the test section. Assuming the small perturbations $\delta M$, $\delta\theta$, and $\delta\theta_a$, Eq. (40) can be expressed as the following state-space representation:

$${}_0^{\mathrm{RL}}\mathfrak{D}_t^{\alpha}\boldsymbol{\xi}(t) = \boldsymbol{A}\boldsymbol{\xi}(t) + \boldsymbol{A}_0\boldsymbol{\xi}(t - h(t)) + \boldsymbol{B}\operatorname{sat}(\boldsymbol{u}(t)), \tag{41}$$

with $\boldsymbol{\xi}^{\mathrm{T}} = [\delta M \ \ \delta\theta \ \ \delta\dot{\theta}]$, $\boldsymbol{A} = \begin{bmatrix} -a & 0 & 0 \\ 0 & 0 & 1 \\ 0 & -\omega^2 & -2\varsigma\omega \end{bmatrix}$, $\boldsymbol{A}_0 = \begin{bmatrix} 0 & ka & 0 \\ 0 & 0 & 0 \\ 0 & 0 & 0 \end{bmatrix}$, and $\boldsymbol{B} = \begin{bmatrix} 0 \\ 0 \\ \omega^2 \end{bmatrix}$.

This example is a special case of the nominal system (14). The following theorem gives a condition to stabilize system (41):

**Theorem 3** If there exist symmetric positive definite matrices $\bar{\boldsymbol{P}}$, $\bar{\boldsymbol{M}}$, $\bar{\boldsymbol{N}}$, matrices $\boldsymbol{U}$, $\boldsymbol{L}$, $\boldsymbol{X}$, a diagonal matrix $\boldsymbol{R}$ with compatible dimensions, and a real scalar $\gamma$ satisfying the conditions (42)−(44):

$$\begin{bmatrix} \boldsymbol{\varXi}_{11} & * & * & * & * \\ \boldsymbol{\varXi}_{21} & \boldsymbol{\varXi}_{22} - \bar{\boldsymbol{Z}} & * & * & * \\ \boldsymbol{\varXi}_{31} & \boldsymbol{\varXi}_{32} & \boldsymbol{\varXi}_{33} & * & * \\ \boldsymbol{0} & \boldsymbol{0} & \boldsymbol{0} & \boldsymbol{\varXi}_{44} & * \\ \boldsymbol{\varXi}_{61} & \boldsymbol{\varXi}_{62} & \boldsymbol{0} & \boldsymbol{0} & \boldsymbol{\varXi}_{66} \end{bmatrix} < 0, \tag{42}$$

$$\begin{bmatrix} \bar{\boldsymbol{P}} & * \\ \boldsymbol{U} - \boldsymbol{L} & \beta {u_0}^2 \end{bmatrix} \geq 0, \tag{43}$$

$$\begin{aligned}
&\left(\bar{\lambda}(\boldsymbol{X}^{-1}\bar{\boldsymbol{P}}\boldsymbol{X}^{-\mathrm{T}}) + \bar{\eta}\bar{\lambda}(\boldsymbol{X}^{-1}\bar{\boldsymbol{M}}\boldsymbol{X}^{-\mathrm{T}})\right)\|\boldsymbol{Q}\|_c^2 + \\
&\quad \left(\frac{\bar{\eta}^2}{2}\bar{\lambda}\left(\boldsymbol{X}^{-1}\bar{\boldsymbol{N}}\boldsymbol{X}^{-\mathrm{T}}\right)\right)\|\dot{\boldsymbol{Q}}\|_c^2 \leq \beta^{-1},
\end{aligned} \tag{44}$$

then applying the controller gain $\boldsymbol{K}=\boldsymbol{U}\boldsymbol{X}^{-\mathrm{T}}$, system (41) is asymptotically stable.

**Proof** We need to follow the same steps as in the proof of Theorem 2 by considering $\bar{\boldsymbol{Z}}=\boldsymbol{C}=\Delta\boldsymbol{A}(t)=\Delta\boldsymbol{A}_{\mathbf{0}}(t)=\Delta\boldsymbol{C}(t)=\mathbf{0}$.

## 6 Numerical examples

Here, the efficiency of the control method is evaluated using two examples.

**Example 1** Assume the uncertain FO system (16) with parameters $\boldsymbol{A}=\begin{bmatrix}-0.6 & 1\\ 1 & 0.4\end{bmatrix}$, $\boldsymbol{A}_0=\begin{bmatrix}0.6 & 0.4\\ 0 & -0.5\end{bmatrix}$, $\boldsymbol{B}=\begin{bmatrix}1\\ 1\end{bmatrix}$, $\boldsymbol{C}=\begin{bmatrix}0.5 & 0.2\\ 0.2 & 0.5\end{bmatrix}$, $\boldsymbol{H}=\begin{bmatrix}0.5 & -0.8\\ 0.5 & 1\end{bmatrix}$, $\boldsymbol{\mathcal{G}}(t)=\begin{bmatrix}\sin t & 0\\ 0 & \cos t\end{bmatrix}$, $u_0=0.5$, $d=0.4$, and $h(t)=0.2+0.4|\sin(t)|$. Furthermore, $\boldsymbol{F}_0=0.1\boldsymbol{A}$, $\boldsymbol{F}_1=0.1\boldsymbol{A}_0$, $\boldsymbol{F}_2=0.1\boldsymbol{C}$, $\gamma=1$, $\beta=0.01$, and $\rho=10$. Solving the LMI conditions in Theorem 2, we obtain the following feasible solutions:
$\bar{\boldsymbol{P}}=\begin{bmatrix}0.0021 & 0.0021\\ 0.0021 & 0.0021\end{bmatrix}$, $\bar{\boldsymbol{M}}=\begin{bmatrix}0.0033 & 0.0032\\ 0.0032 & 0.0032\end{bmatrix}$, $\bar{\boldsymbol{N}}=1.0\mathrm{e}^{-6}\begin{bmatrix}0.2641 & -0.0830\\ -0.0830 & 0.1629\end{bmatrix}$, $\bar{\boldsymbol{Z}}=1.0\mathrm{e}^{-4}\begin{bmatrix}0.6044 & 0.4854\\ 0.4854 & 0.5784\end{bmatrix}$, $\boldsymbol{X}=1.0\mathrm{e}^{-4}\begin{bmatrix}0.6222 & 0.4750\\ 0.4102 & 0.6589\end{bmatrix}$, $R=3.6577\mathrm{e}^{-7}$, $\boldsymbol{L}=1.0\mathrm{e}^{-5}\begin{bmatrix}-0.1068 & -0.1058\end{bmatrix}$, $q=1.0389\mathrm{e}^{-5}$, $\boldsymbol{U}=\begin{bmatrix}-0.0022 & -0.0022\end{bmatrix}$.

Considering different initial conditions, namely $\boldsymbol{\xi}_0=[-0.3\ \ 0.6]^{\mathrm{T}}$, $[0.2\ \ -0.1]^{\mathrm{T}}$, and $[0.8\ \ -0.8]^{\mathrm{T}}$, the open-loop system is unstable as depicted in Fig. 1. The state feedback controller gains are determined using the proposed controller algorithm as $\boldsymbol{K}=[-9.8306\ \ -10.2205]$. Furthermore, Figs. 2 and 3 present the behaviors of the overall system for different values of $\alpha=0.9$ and 0.7, and with different initial conditions $\boldsymbol{\xi}_0=[-0.3\ \ 0.6]^{\mathrm{T}}$, $[0.2\ \ -0.1]^{\mathrm{T}}$, and $[0.8\ \ -0.8]^{\mathrm{T}}$. In addition, we can see that decreasing the FO value $\alpha$ increases the response settling time. Next, we maximize the stability radius $\rho$, so that system (16) is robustly stable. Assuming the delay $h(t)$ mentioned above, we have $\bar{h}=0.6$. Now, we fix the delay and parameter $\rho$ varies until the conditions in Theorem 2 hold. The controller gain is $\boldsymbol{K}=\begin{bmatrix}-13.2770 & -13.3645\end{bmatrix}$ for $\rho=55$. As expected, large values of $\rho$ imply large values of the control input.

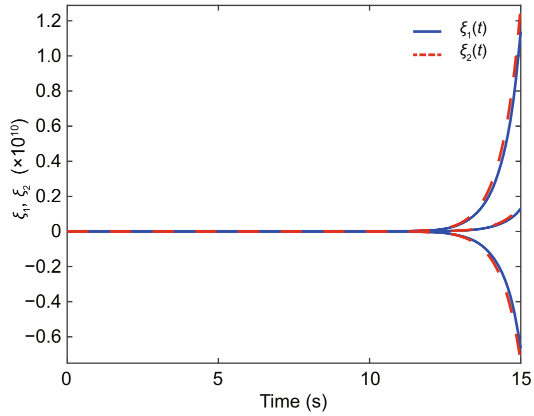


**Fig. 1 The open-loop system states of example 1 with $\alpha=0.9$ for different initial conditions ($\boldsymbol{\xi}_0=[-0.3\ \ 0.6]^{\mathrm{T}}$, $[0.2\ \ -0.1]^{\mathrm{T}}$, and $[0.8\ \ -0.8]^{\mathrm{T}}$)**

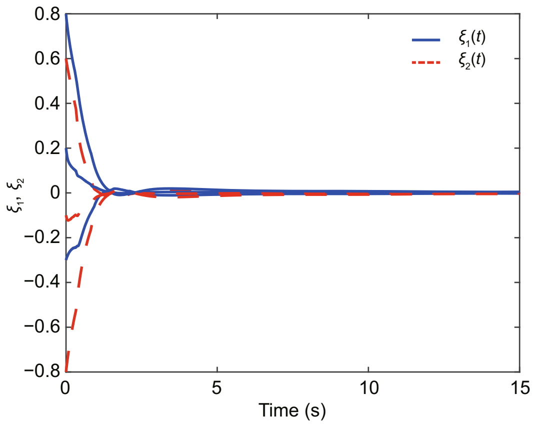


**Fig. 2 The closed-loop system states of example 1 with $\alpha=0.9$ for different initial conditions ($\boldsymbol{\xi}_0=[-0.3\ \ 0.6]^{\mathrm{T}}$, $[0.2\ \ -0.1]^{\mathrm{T}}$, and $[0.8\ \ -0.8]^{\mathrm{T}}$)**

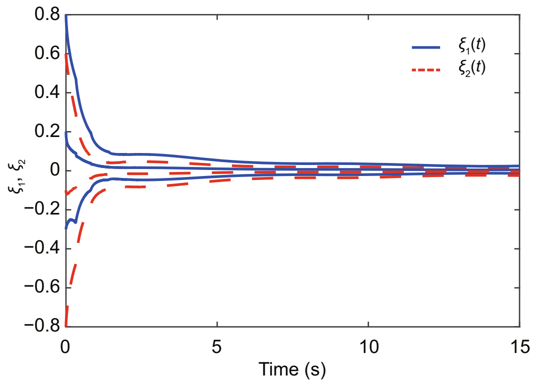


**Fig. 3 The states of example 1 with $\alpha=0.7$ for different initial conditions ($\boldsymbol{\xi}_0=[-0.3\ \ 0.6]^{\mathrm{T}}$, $[0.2\ \ -0.1]^{\mathrm{T}}$, and $[0.8\ \ -0.8]^{\mathrm{T}}$)**

**Example 2** The stabilization criterion for the wind tunnel is now studied with the following dynamical model:

$$
{}_0^{\mathrm{RL}}\mathfrak{D}_t^{\alpha}\boldsymbol{\xi}(t) = \begin{bmatrix} -a & 0 & 0 \\ 0 & 0 & 1 \\ 0 & -\omega^2 & -2\varsigma\omega \end{bmatrix} \boldsymbol{\xi}(t) + \begin{bmatrix} 0 & k_a & 0 \\ 0 & 0 & 0 \\ 0 & 0 & 0 \end{bmatrix} \boldsymbol{\xi}(t-h(t)) + \begin{bmatrix} 0 \\ 0 \\ \omega^2 \end{bmatrix} \mathrm{sat}(\boldsymbol{u}(t)),
$$

with $\boldsymbol{\xi}^{\mathrm{T}} = [\delta M \quad \delta\theta \quad \delta\dot{\theta}]$. Assuming $1/a = 1.946$ s, $\omega = 6$ rad/s, $\varsigma = 0.8$, and $k_a = -0.0117$ deg$^{-1}$ (Manitius, 1984), the example is a particular case of the nominal system (16). Then, letting $u_0 = 1$, $h(t) = 0.4|\sin t| + 0.2$, $d = 0.4$, $\gamma = 1$, $\beta = 0.1$, and $\rho = 1$, we obtain the following solutions:

$$
\bar{\boldsymbol{P}} = \begin{bmatrix} 0.3017 & 0 & 0 \\ 0 & 0.2492 & -0.0114 \\ 0 & -0.0114 & 0.3318 \end{bmatrix},
$$

$$
\bar{\boldsymbol{M}} = \begin{bmatrix} 0.2147 & 0 & 0 \\ 0 & 0.2485 & -0.0923 \\ 0 & -0.0923 & 0.2490 \end{bmatrix},
$$

$$
\bar{\boldsymbol{N}} = \begin{bmatrix} 0.3712 & 0 & 0 \\ 0 & 0.0901 & -0.0216 \\ 0 & -0.0216 & 0.1570 \end{bmatrix},
$$

$$
\boldsymbol{X} = \begin{bmatrix} 0.3906 & 0 & 0 \\ 0 & 0.1060 & -0.1672 \\ 0 & -0.0107 & 0.2030 \end{bmatrix},
$$

$$
\boldsymbol{L} = 1.0\mathrm{e}^{-4}\,[0 \quad 0.1809 \quad -0.1797],
$$

$$
\boldsymbol{U} = [0 \quad 0.0621 \quad 0.0256],\ R = 1.0774\mathrm{e}^{-4}.
$$

Using the proposed control algorithm, we obtain $\boldsymbol{K} = [0.0001 \quad 0.2716 \quad 0.1559]$. The simulation results for $\alpha = 0.9$ are shown in Fig. 4, indicating good performances of the controller.

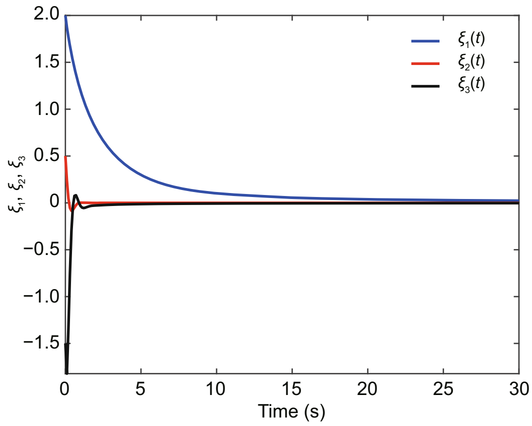


**Fig. 4 The states of example 2 with $\alpha = 0.9$ (References to color refer to the online version of this figure)**

## 7 Conclusions

This paper studied the robust stability of uncertain neutral-type fractional-order systems with actuator saturation. The Lyapunov–Krasovskii functional was constructed to determine the criteria with the help of linear matrix inequalities. A state feedback controller was designed to stabilize this system, and an algorithm for computing the stabilizing gains was proposed via the CCL method. Two examples demonstrated the applicability of the new method.

## Contributors

Zahra Sadat AGHAYAN and Alireza ALFI conceived the concept. Zahra Sadat AGHAYAN designed the software and drafted the paper. J. A. TENREIRO MACHADO helped research literature. Alireza ALFI and J. A. TENREIRO MACHADO revised and finalized the paper.

## Compliance with ethics guidelines

Zahra Sadat AGHAYAN, Alireza ALFI, and J. A. TENREIRO MACHADO declare that they have no conflict of interest.

## References

Aghayan ZS, Alfi A, Tenreiro Machado JA, 2020. Stability analysis of fractional order neutral-type systems considering time varying delays, nonlinear perturbations, and input saturation. *Math Methods Appl Sci*, 43(17):10332-10345. https://doi.org/10.1002/mma.6701

Alaviyan Shahri ES, Alfi A, Tenreiro Machado JA, 2018a. Robust stability and stabilization of uncertain fractional order systems subject to input saturation. *J Vibr Contr*, 24(16):3676-3683. https://doi.org/10.1177/1077546317708927

Alaviyan Shahri ES, Alfi A, Tenreiro Machado J, 2018b. Stability analysis of a class of nonlinear fractional-order systems under control input saturation. *Int J Robust Nonl Contr*, 28(7):2887-2905. https://doi.org/10.1002/rnc.4055

Altun Y, Tunç C, 2019. On exponential stability of solutions of nonlinear neutral differential systems with discrete and distributed variable lags. *Nonl Stud*, 26(2):455-466.

Badri P, Sojoodi M, 2019a. LMI-based robust stability and stabilization analysis of fractional-order interval systems with time-varying delay. https://arxiv.org/abs/1909.08415v1

Badri P, Sojoodi M, 2019b. Robust stabilisation of fractional-order interval systems via dynamic output feedback: an LMI approach. *Int J Syst Sci*, 50(9):1718-1730. https://doi.org/10.1080/00207721.2019.1622817

Badri P, Sojoodi M, 2019c. Stability and stabilization of fractional-order systems with different derivative orders: an LMI approach. *Asian J Contr*, 21(5):2270-2279. https://doi.org/10.1002/asjc.1847

Baleanu D, Jajarmi A, Asad JH, 2019a. Classical and fractional aspects of two coupled pendulums. *Roman Rep Phys*, 71(1):103.

Baleanu D, Sajjadi SS, Jajarmi A, et al., 2019b. New features of the fractional Euler-Lagrange equations for a physical system within non-singular derivative operator. *Eur Phys J Plus*, 134(4):181. https://doi.org/10.1140/epjp/i2019-12561-x

Barbarossa M, Hadeler K, Kuttler C, 2014. State-dependent neutral delay equations from population dynamics. *J Math Biol*, 69(4):1027-1056. https://doi.org/10.1007/s00285-014-0821-8

Binazadeh T, Yousefi M, 2018. Asymptotic stabilization of a class of uncertain nonlinear time-delay fractional-order systems via a robust delay-independent controller. *J Vibr Contr*, 24(19):4541-4550. https://doi.org/10.1177/1077546317729956

Chartbupapan W, Bagdasar O, Mukdasai K, 2020. A novel delay-dependent asymptotic stability conditions for differential and Riemann–Liouville fractional differential neutral systems with constant delays and nonlinear perturbation. *Mathematics*, 8(1):82. https://doi.org/10.3390/math8010082

Chen WS, Dai H, Song YF, et al., 2017. Convex Lyapunov functions for stability analysis of fractional order systems. *IET Contr Theory Appl*, 11(7):1070-1074. https://doi.org/10.1049/iet-cta.2016.0950

Dubey VP, Kumar R, Kumar D, et al., 2020. An efficient computational scheme for nonlinear time fractional systems of partial differential equations arising in physical sciences. *Adv Differ Equat*, 2020(1):46. https://doi.org/10.1186/s13662-020-2505-6

Elahi A, Alfi A, 2017. Finite-time $H_\infty$ control of uncertain networked control systems with randomly varying communication delays. *ISA Trans*, 69:65-88. https://doi.org/10.1016/j.isatra.2017.04.004

El Fezazi N, El Haoussi F, Tissir EH, et al., 2017. Robust stabilization using LMI techniques of neutral time-delay systems subject to input saturation. *J Phys Conf Ser*, 783(1):012031. https://doi.org/10.1088/1742-6596/783/1/012031

Gu KQ, Kharitonov VL, Chen J, 2003. Stability of Time-Delay Systems. Birkhäuser, Boston, USA. https://doi.org/10.1007/978-1-4612-0039-0

Han QL, 2005. Stability analysis for a partial element equivalent circuit (PEEC) model of neutral type. *Int J Circ Theory Appl*, 33(4):321-332. https://doi.org/10.1002/cta.323

He BB, Zhou HC, Kou CH, 2020. Controllability of fractional-order damped systems with time-varying delays in control. *Front Inform Technol Electron Eng*, 21(6):844-855. https://doi.org/10.1631/FITEE.1900736

Hu BX, Song QK, Zhao ZJ, 2020. Robust state estimation for fractional-order complex-valued delayed neural networks with interval parameter uncertainties: LMI approach. *Appl Math Comput*, 373:125033. https://doi.org/10.1016/j.amc.2020.125033

Hu TT, He Z, Zhang XJ, et al., 2020. Finite-time stability for fractional-order complex-valued neural networks with time delay. *Appl Math Comput*, 365:124715. https://doi.org/10.1016/j.amc.2019.124715

Kilbas AA, Bonilla B, Trukhillo K, 2000. Fractional integrals and derivatives and differential equations of fractional order in weighted spaces of continuous functions. *Dokl Nats Akad Nauk Belar*, 44(6):18-22.

Kilbas AA, Srivastava HM, Trujillo JJ, 2006. Theory and Applications of Fractional Differential Equations. Elsevier, Amsterdam, the Netherlands.

Li JD, Wu ZB, Huang NJ, 2019. Asymptotical stability of Riemann–Liouville fractional-order neutral-type delayed projective neural networks. *Neur Process Lett*, 50(1):565-579. https://doi.org/10.1007/s11063-019-10050-8

Lien CH, Yu KW, Lin YF, et al., 2008. Global exponential stability for uncertain delayed neural networks of neutral type with mixed time delays. *IEEE Trans Syst Man Cybern Part B (Cybern)*, 38(3):709-720. https://doi.org/10.1109/TSMCB.2008.918564

Liu MY, Dassios I, Milano F, 2019. On the stability analysis of systems of neutral delay differential equations. *Circ Syst Signal Process*, 38(4):1639-1653. https://doi.org/10.1007/s00034-018-0943-0

Liu S, Jiang W, Li XY, et al., 2016. Lyapunov stability analysis of fractional nonlinear systems. *Appl Math Lett*, 51:13-19. https://doi.org/10.1016/j.aml.2015.06.018

Manitius A, 1984. Feedback controllers for a wind tunnel model involving a delay: analytical design and numerical simulation. *IEEE Trans Autom Contr*, 29(12):1058-1068. https://doi.org/10.1109/TAC.1984.1103436

Mohsenipour R, Fathi Jegarkandi M, 2019. Robust stability analysis of fractional-order interval systems with multiple time delays. *Int J Robust Nonl Contr*, 29(6):1823-1839. https://doi.org/10.1002/rnc.4461

Pahnehkolaei SMA, Alfi A, Machado JAT, 2017a. Chaos suppression in fractional systems using adaptive fractional state feedback control. *Chaos Sol Fract*, 103:488-503. https://doi.org/10.1016/j.chaos.2017.06.003

Pahnehkolaei SMA, Alfi A, Machado JAT, 2017b. Uniform stability of fractional order leaky integrator echo state neural network with multiple time delays. *Inform Sci*, 418-419:703-716. https://doi.org/10.1016/j.ins.2017.08.046

Pahnehkolaei SMA, Alfi A, Machado JAT, 2019a. Delay-dependent stability analysis of the QUAD vector field fractional order quaternion-valued memristive uncertain neutral type leaky integrator echo state neural networks. *Neur Netw*, 117:307-327. https://doi.org/10.1016/j.neunet.2019.05.015

Pahnehkolaei SMA, Alfi A, Machado JAT, 2019b. Stability analysis of fractional quaternion-valued leaky integrator echo state neural networks with multiple time-varying delays. *Neurocomputing*, 331:388-402. https://doi.org/10.1016/j.neucom.2018.11.021

Petersen IR, 1987. A stabilization algorithm for a class of uncertain linear systems. *Syst Contr Lett*, 8(4):351-357. https://doi.org/10.1016/0167-6911(87)90102-2

Pu YF, Wang J, 2020. Fractional-order global optimal backpropagation machine trained by an improved fractional-order steepest descent method. *Front Inform Technol Electron Eng*, 21(6):809-833. https://doi.org/10.1631/FITEE.1900593

Ren HL, Zong GD, Hou LL, et al., 2017. Finite-time resilient decentralized control for interconnected impulsive switched systems with neutral delay. *ISA Trans*, 67:19-29. https://doi.org/10.1016/j.isatra.2017.01.013

Shahri ESA, Alfi A, Machado JAT, 2015. An extension of estimation of domain of attraction for fractional order linear system subject to saturation control. *Appl Math Lett*, 47:26-34.
https://doi.org/10.1016/j.aml.2015.02.020

Shahri ESA, Alfi A, Tenreiro Machado JA, 2017. Stabilization of fractional-order systems subject to saturation element using fractional dynamic output feedback sliding mode control. *J Comput Nonl Dynam*, 12(3):031014.
https://doi.org/10.1115/1.4035196

Shahri ESA, Alfi A, Machado JAT, 2020. Lyapunov method for the stability analysis of uncertain fractional-order systems under input saturation. *Appl Math Model*, 81:663-672. https://doi.org/10.1016/j.apm.2020.01.013

Song S, Park JH, Zhang BY, et al., 2020. Adaptive hybrid fuzzy output feedback control for fractional-order nonlinear systems with time-varying delays and input saturation. *Appl Math Comput*, 364:124662.
https://doi.org/10.1016/j.amc.2019.124662

Udhayakumar K, Rakkiyappan R, Cao JD, et al., 2020. Mittag–Leffler stability analysis of multiple equilibrium points in impulsive fractional-order quaternion-valued neural networks. *Front Inform Technol Electron Eng*, 21(2):234-246.
https://doi.org/10.1631/FITEE.1900409

Valério D, Trujillo JJ, Rivero M, et al., 2013. Fractional calculus: a survey of useful formulas. *Eur Phys J Spec Top*, 222(8):1827-1846.
https://doi.org/10.1140/epjst/e2013-01967-y

Witrant E, 2005. Stabilisation des Systèmes Commandés par Réseaux (Stability of Networked Control Systems). PhD Thesis, Institut National Polytechnique, Grenoble, France (in French).

Yang HY, Yang YZ, Han FJ, et al., 2019. Containment control of heterogeneous fractional-order multi-agent systems. *J Franklin Inst*, 356(2):752-765.
https://doi.org/10.1016/j.jfranklin.2017.09.034

Zhang FZ, 2006. The Schur Complement and Its Applications. Springer Science & Business Media, Boston, USA. https://doi.org/10.1007/b105056

Zhang S, Liu L, Cui XS, 2019. Robust FOPID controller design for fractional-order delay systems using positive stability region analysis. *Int J Robust Nonl Contr*, 29(15):5195-5212. https://doi.org/10.1002/rnc.4667

Zhang XF, Chen YQ, 2018. Admissibility and robust stabilization of continuous linear singular fractional order systems with the fractional order $\alpha$: the $0 < \alpha < 1$ case. *ISA Trans*, 82:42-50.
https://doi.org/10.1016/j.isatra.2017.03.008

Zhang Y, Sun HG, Stowell HH, et al., 2017. A review of applications of fractional calculus in Earth system dynamics. *Chaos Sol Fract*, 102:29-46.
https://doi.org/10.1016/j.chaos.2017.03.051

Zhu CH, Li XD, Wang KN, 2020. An anti-windup approach for nonlinear impulsive system subject to actuator saturation. *Chaos Sol Fract*, 133:109658.
https://doi.org/10.1016/j.chaos.2020.109658